Spatial coherence in strongly scattering media

Romain Pierrat, Jean-Jacques Greffet, and Rémi Carminati

Laboratoire d'Énergétique Moléculaire et Macroscopique, Combustion, École Centrale Paris, Centre National de la Recherche Scientifique, 92295 Châtenay-Malabry cedex, France

Rachid Elaloufi

Department of Computer Science, University College London, London WC1E6BT, United Kingdom

Received February 10, 2005; revised manuscript received April 22, 2005; accepted April 28, 2005

We study the spatial coherence of an optical beam in a strongly scattering medium confined in a slab geometry. Using the radiative transfer equation, we study numerically the behavior of the transverse spatial coherence length in the different transport regimes. Transitions from the ballistic to the diffusive regimes are clearly identified. © 2005 Optical Society of America

OCIS codes: 030.1640, 170.5280, 170.7050, 290.4210.

1. INTRODUCTION

Light transport in the multiple-scattering regime has become a very active field owing to the rapid development of biomedical imaging techniques using visible or near-infrared light.[1] In many cases, modeling the intensity profile (in space and time) is sufficient in order to analyze the images or to improve the experimental setups. Most of the practical approaches rely on the diffusion approximation, which is valid at large length and time scales (compared with the transport mean-free path and the collision time).[2]

In some cases, knowledge of the spatial coherence properties of light propagating through a turbid medium is of primary importance, e.g., to characterize the beam quality,[3] to analyze speckle correlations,[1,3] or to model dynamic experiments based on light fluctuations induced by the motion of the scatterers, as in diffusing-wave spectroscopy.[4] The spatial coherence length can be used to characterize the quality of a beam transmitted through a turbulent atmosphere.[5–7] The beam quality and the size of the spatially coherent illuminating spot are also key parameters in optical coherence tomography in media where multiple scattering plays a role.[8]

In this work, we study the spatial coherence of light propagating through a slab of scattering medium, whose properties are similar to that of biological tissues. We introduce a practical way to compute the field spatial correlation function and the spatial coherence length, both inside and outside the medium (in transmission or reflection). We use a numerical solution of the radiative transfer equation (RTE) to calculate the specific intensity $I_\nu(\mathbf{r},\mathbf{u})$ in a slab geometry, from which we derive the cross-spectral density and the spatial coherence length. With this approach, we study the evolution of the spatial coherence in the scattering medium. In particular, we discuss the crossover between the ballistic and the diffusive regimes.

2. TRANSPORT EQUATION FOR FIELD CORRELATION

In this section, we recall the relationship between the specific intensity and the cross-spectral density. Different forms of this relationship have been derived previously.[3,9–14] We introduce the RTE as a transport equation for the specific intensity, defined as the three-dimensional Wigner transform of the field.

A. Basic Concepts of Spatial Coherence Theory

We consider a scattering medium, described statistically by a random process and illuminated by a monochromatic field of frequency ν. The scattered field $u(\mathbf{r},t)=u(\mathbf{r})\times\exp(-2i\pi\nu t)$ is itself a random variable. We use the scalar approximation so that we neglect polarization effects. The second-order spatial coherence properties of the field are characterized by the cross-spectral density[15]

$$W(\mathbf{r}_1,\mathbf{r}_2,\nu)=\int_{-\infty}^{+\infty}\langle u(\mathbf{r}_1,t)u^*(\mathbf{r}_2,t+\tau)\rangle\exp[2i\pi\nu\tau]\mathrm{d}\tau, \quad (1)$$

where * denotes the complex conjugate and $\langle\cdots\rangle$ denotes an average over an ensemble of realizations of the scattering medium. The field is assumed to be statistically stationary, so that W is independent of time. W is a measure of the field spatial correlation at a given frequency. In a scattering random medium, an exact transport equation for W can be derived from the wave equation.[3,16] This equation, known as the Bethe–Salpeter equation, is an integral equation whose kernel is difficult to compute explicitly. We will therefore introduce an approximation to this transport equation, known as the RTE.

In the following, we introduce the new variables $\mathbf{r}=(\mathbf{r}_1+\mathbf{r}_2)/2$ and $\boldsymbol{\rho}=\mathbf{r}_2-\mathbf{r}_1$, and we omit the frequency ν for the sake of brevity. If the random medium is statistically homogeneous and isotropic, the cross-spectral density depends on $\rho=\|\mathbf{r}_2-\mathbf{r}_1\|$ only. One usually defines the spatial

coherence length l_{coh} as the FWHM of the degree of spatial coherence $w(\rho)=W(\rho)/W(0)$. If the beam is spatially coherent, the correlation function is constant, and thus l_{coh} tends to infinity. By contrast, if the beam is incoherent, the correlation function is null for $\rho\neq 0$, and thus l_{coh} is null. In other situations, the beam is said to be partially coherent.

B. Link between the Specific Intensity and the Cross-Spectral Density

In this subsection, we introduce the specific intensity, which can be defined as follows[2,3,16,17]:

$$W(\mathbf{r},\boldsymbol{\rho})=\int_{4\pi} I_\nu(\mathbf{r},\mathbf{u})\exp(ik\mathbf{u}\cdot\boldsymbol{\rho})\mathrm{d}\Omega, \tag{2}$$

where $k=2\pi/\lambda$ is the wavenumber in the medium. Note that Eq. (2) can be inverted to obtain the specific intensity in the form of a Wigner transform of the field. One obtains Walther's formula[9] as shown in Appendix A. Starting from the Bethe–Salpeter equation, it has been shown by many authors that I_ν verifies the RTE.[2,3,16–18] The RTE is a Boltzmann-type transport equation, which, in the steady-state regime, can be written as

$$\mathbf{u}\cdot\boldsymbol{\nabla}_{\mathbf{r}} I_\nu(\mathbf{r},\mathbf{u})=-(\mu_a+\mu_s)I_\nu(\mathbf{r},\mathbf{u})+\frac{\mu_s}{4\pi}\int_{4\pi} p(\mathbf{u},\mathbf{u}')I_\nu(\mathbf{r},\mathbf{u}')\mathrm{d}\Omega'. \tag{3}$$

In this equation, μ_s is the scattering coefficient, and μ_a is the absorption coefficient. The associated scattering and absorption mean-free paths are $l_s=\mu_s^{-1}$ and $l_a=\mu_a^{-1}$. We also define the transport mean-free path $l^*=l_s/(1-g)$, where $g=\langle\cos\theta\rangle$ is the average cosine of the scattering angle.[2] $p(\mathbf{u},\mathbf{u}')$ is the phase function. l^* can be interpreted as the average distance for collimated light to become isotropic because of scattering. The extinction coefficient is given by $\mu_e=\mu_s+\mu_a$, and $a=\mu_s/\mu_e$ is the albedo.

This equation was first introduced in astrophysics as a phenomenological equation.[19] It was derived from a local radiative energy balance, in which the specific intensity plays the role of a local and directional energy flux. Although the specific intensity, defined in radiometry, is always positive, the expression defined in Eq. (2) can take negative values. It can be shown that in the limit $\lambda\to 0$ the specific intensity is always positive and can be interpreted as a local energy flux.[15] Nevertheless, this limit is not necessary for Eqs. (2) and (3) to be valid.[3,16] The specific intensity takes negative values when the wave nature of the field becomes relevant, as discussed in Ref. 3. Littlejohn and Winston[20,21] have shown that the energy flux computed using the Wigner transform is always positive. Moreover, the existence of negative values of I_ν does not prevent the RTE from being considered a radiometric transport equation.

3. PARTICULAR CASE: SLAB GEOMETRY

A. Geometry of the System

The system is described in Fig. 1. It consists of a statistically homogeneous scattering slab of thickness L, which is infinite along the x and y axes. We will refer to this medium as medium **2**. The medium $z<0$ is denoted by **1**, and the medium $z>L$ is denoted by **3**. The real parts of the refractive indices are n_1, n_2, and n_3, respectively, for media **1**, **2**, and **3**. The angles θ and φ denote the spherical coordinate angles. The slab is illuminated from the left by a plane wave at normal incidence. In this study we have considered $n_1=n_3=1$ and $n_2\geqslant 1$.

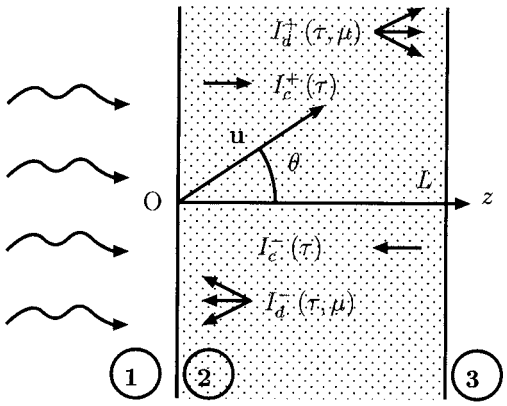

Fig. 1. Geometry of the system. Medium **2** is a scattering slab of thickness L illuminated from the left by a plane wave at normal incidence. The notations used to decompose the specific intensity into ballistic and diffuse components propagating in the forward and backward directions are indicated.

B. Cross-Spectral Density in a Slab Geometry

The geometry is translationally invariant along x and y and is rotationally invariant around the z axis. Assuming that the phase function depends only on $\mathbf{u}\cdot\mathbf{u}'$, the specific intensity depends on z and $\mu=\cos\theta$ only. Moreover, we are interested in the cross-spectral density in a plane perpendicular to the direction of propagation (the x–y plane in our case). So the vector $\boldsymbol{\rho}$ in Eq. (2) belongs to a plane z = constant. In this plane, the cross-spectral density depends only on ρ. Equation (2) becomes

$$W(z,\boldsymbol{\rho})=\int I_\nu(z,\mu,\varphi)\exp(ik\boldsymbol{\rho}\cdot\mathbf{u})\mathrm{d}\mu\mathrm{d}\varphi. \tag{4}$$

Since $\boldsymbol{\rho}\cdot\mathbf{u}=\rho u_\perp\cos\varphi$ where $u_\perp$ is the projection of $\mathbf{u}$ on the x–y plane, we recognize a Bessel function of order 0 defined by

$$\mathcal{J}_0(x)=\frac{1}{2\pi}\int_0^{2\pi}\exp(ix\cos\varphi)\mathrm{d}\varphi. \tag{5}$$

We can cast the cross-spectral density in the form

$$W(z,\rho)=\int_{-1}^{+1} I_\nu(z,\mu)\mathcal{J}_0\left(\frac{2\pi}{\lambda}\rho\sqrt{1-\mu^2}\right)\mathrm{d}\mu, \tag{6}$$

where $u_\perp=\sqrt{1-\mu^2}$. We used the fact that $I_\nu(z,\mu,\varphi)$ does not depend on φ, and we introduced $I_\nu(z,\mu)=\int_0^{2\pi} I_\nu(z,\mu,\varphi)\mathrm{d}\varphi=2\pi I_\nu(z,\mu,\varphi)$. Equation (6) allows us to derive the cross-spectral density in a plane z = constant from the specific intensity calculated from the RTE. Owing to the linearity of the integral, we can easily split the cross-spectral density corresponding to the specific intensity propagating in the forward direction (i.e., $\mu>0$) and

the one corresponding to the specific intensity in the backward direction (i.e., $\mu<0$).

Two particular cases are important to analyze the numerical results in Section 4. For a collimated specific intensity [i.e., $I_\nu(z,\mu)=I_\nu(z)\delta(\mu\pm1)$], the spatial correlation function is constant, and the coherence length tends to infinity. We retrieve the well-known coherence property of the collimated component, which is often called the coherent component. For an isotropic specific intensity [i.e., $I_\nu(z,\mu)=I_\nu(z)$], Eq. (6) yields

$$W(z,\rho)=2I_\nu(z)\mathrm{sinc}\left(\frac{2\pi\rho}{\lambda}\right). \tag{7}$$

The details of calculation are given in Appendix B. In this case, the coherence length does not depend on z, and the FWHM is given by

$$l_{coh}\approx 0.3\lambda. \tag{8}$$

This expression for the coherence length is a characteristic of isotropic radiation. The same result is obtained for blackbody radiation.[15] As given in Appendix B, this result is also valid when one considers only the propagation of light in the forward direction (i.e., by applying the operator $\int_0^{+1}\ldots d\mu$) or in the backward direction (i.e., by applying the operator $\int_{-1}^{0}\ldots d\mu$).

The purpose of this paper is to study the transition between these two regimes in a strongly scattering medium.

C. Radiative Transfer Equation

The transport equation for I_ν in a steady-state regime for a slab geometry can be written as[19]

$$\mu\frac{\partial}{\partial\tau}I_\nu(\tau,\mu)=-I_\nu(\tau,\mu)+\frac{a}{2}\int_{-1}^{+1}p(\mu,\mu')I_\nu(\tau,\mu')d\mu'. \tag{9}$$

In this equation, both the specific intensity I_ν and the phase function p are integrated over the azimuthal angle φ. We have introduced the dimensionless distance $\tau=\mu_e z$. The optical thickness is given by $L^*=\mu_e L$.

The validity of Eq. (9) in slab geometries has been studied by comparison with rigorous electromagnetic numerical solutions of the multiple-scattering problem.[22] It has been shown that it is valid for both thick and thin slabs (even for thickness of the order of one wavelength). Equation (9) can be solved numerically using a discrete-ordinate method.[23,24] The boundary conditions at the slab interfaces are taken into account rigorously using Fresnel reflection and transmission factors. In the following, the expression of the specific intensity in the slab is calculated from Eq. (9).

4. NUMERICAL RESULTS

A. Collimated and Diffuse Beams

The spatial coherence of a collimated beam is very large. By contrast, an isotropic specific intensity yields a coherence length of 0.3λ. It will be useful to split the specific intensity into two components, collimated and diffuse, in order to study their contribution to the spatial coherence.

First, we solve the RTE in a slab geometry to obtain $I_\nu(\tau,\mu)$. Then, using Eq. (6), we compute the cross-spectral density $W(\tau,\rho)$, whose FWHM yields the transverse coherence length. We see in Fig. 2(a) that when τ increases the coherence length decreases. The coherence length is large close to the medium interface due to the contribution of the ballistic component (propagating in the forward direction). The contribution of the ballistic component decreases exponentially with increasing τ due to scattering and absorption. We also represent in Fig. 2(b) the degree of spatial coherence (i.e., the normalized field correlation function) $w(\tau,\rho)$ inside the scattering medium **2**, versus ρ, and the normalized distance from the medium interface $\tau=\mu_e z$. In this example, the full radiation field is taken into account (with both a forward field propagating toward $z>0$ and a backscattered field). We see that, at a large depth inside the medium, the correlation function exhibits the sinc $(2\pi\rho/\lambda)$ structure characteristic of isotropic radiation. In this case, the transport regime is diffusive.

We also need to separate the specific intensity propagating in the forward direction (i.e., $z>0$) from the one

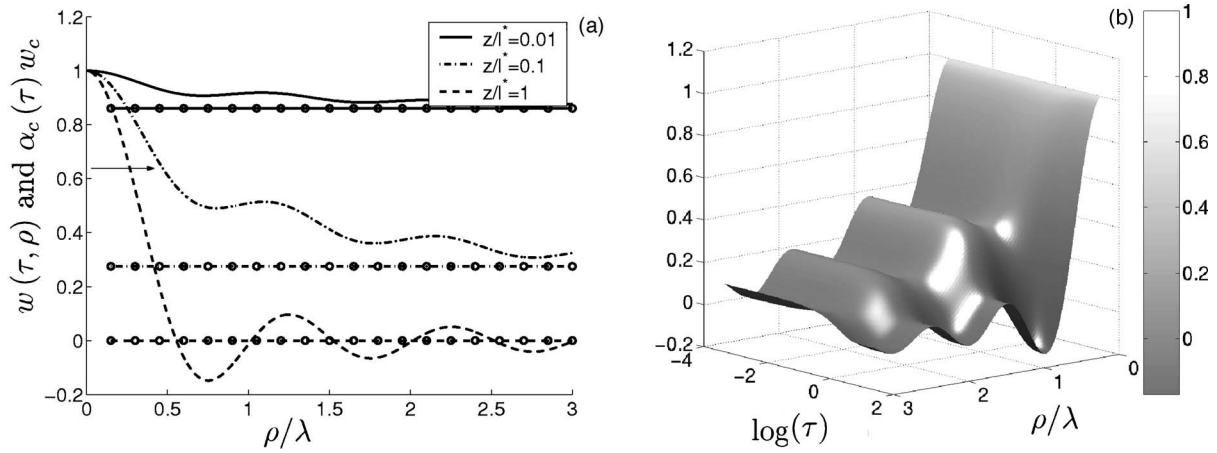

Fig. 2. Degree of spatial coherence $w(\tau,\rho)$ inside a semi-infinite scattering medium versus the normalized distance from the medium interface τ and the distance ρ between the two observation points. The scattering medium is described by a Henyey–Greenstein phase function with $g=0.90$ and an albedo $a=0.98$. (a) Circles correspond to $\alpha_c(\tau)w_c$, and the arrow indicates an example of FWHM for the diffuse component only and is reported on Fig. 3.

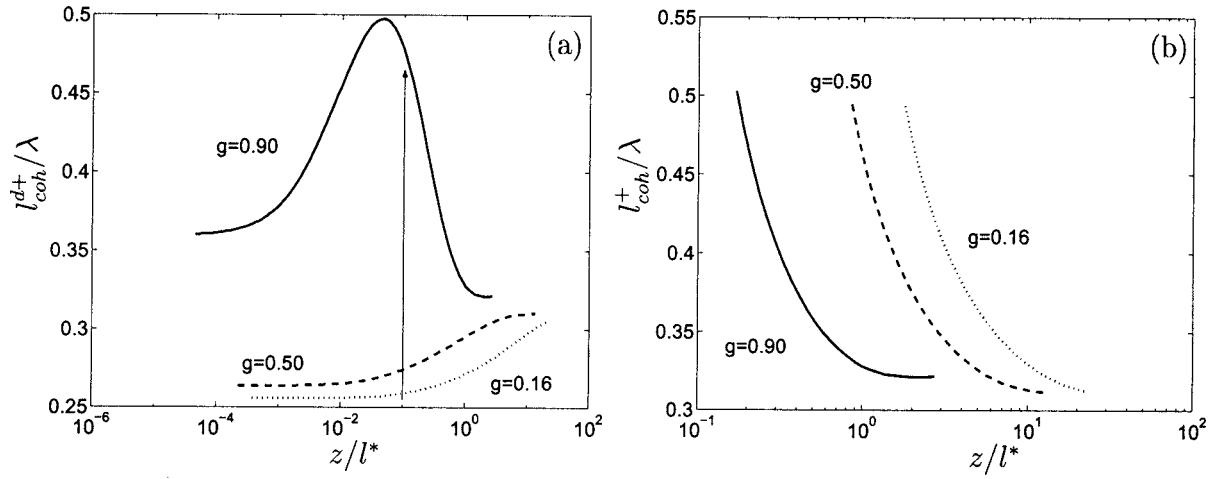

Fig. 3. Spatial coherence length (normalized by the wavelength) of (a) the diffuse radiation and (b) the diffuse and ballistic radiation propagating in the forward direction inside a semi-infinite scattering medium versus the normalized distance z/l^* from the slab interface, where l^* is the transport mean-free path. The scattering medium is described by a Henyey–Greenstein phase function with different values of the anisotropy factor g, an albedo $a=0.98$, and a refractive index $n_2=1$. The arrow indicates an example of FWHM for the scattered part only and is reported on Fig. 2.

propagating in the backward direction (i.e., $z<0$). In this section, we omit the subscript ν for the sake of simplicity. We define

$$I(\tau,\mu)=I_c^+(\tau)\delta(\mu-1)+I_c^-(\tau)\delta(\mu+1)+I_d(\tau,\mu), \quad (10)$$

where

$$I_d^+(\tau,\mu)=I_d(\tau,\mu>0),$$

$$I_d^-(\tau,\mu)=I_d(\tau,\mu<0). \quad (11)$$

These notations are illustrated in Fig. 1. Concerning the cross-spectral density, we introduce the collimated (W_c) and the diffuse (W_d) components:

$$W_c^+(\tau)=I_c^+(\tau),$$

$$W_c^-(\tau)=I_c^-(\tau),$$

$$W_c(\tau)=W_c^+(\tau)+W_c^-(\tau), \quad (12)$$

$$W_d^+(\tau,\rho)=\int_0^{+1} I_d^+(\tau,\mu)\mathcal{J}_0\left(\frac{2\pi}{\lambda}\rho\sqrt{1-\mu^2}\right)\mathrm{d}\mu,$$

$$W_d^-(\tau,\rho)=\int_{-1}^{0} I_d^-(\tau,\mu)\mathcal{J}_0\left(\frac{2\pi}{\lambda}\rho\sqrt{1-\mu^2}\right)\mathrm{d}\mu,$$

$$W_d(\tau,\rho)=W_d^+(\tau,\rho)+W_d^-(\tau,\rho). \quad (13)$$

Inserting Eq. (10) into Eq. (6) yields

$$\frac{W(\tau,\rho)}{W(\tau,0)}=\frac{W_c(\tau)}{W_c(\tau)}\frac{W_c(\tau)}{W_c(\tau)+W_d(\tau,0)}+\frac{W_d(\tau,\rho)}{W_d(\tau,0)}\frac{W_d(\tau,0)}{W_c(\tau)+W_d(\tau,0)}. \quad (14)$$

We can cast Eq. (14) in the form

$$w(\tau,\rho)=w_c\alpha_c(\tau)+w_d(\tau,\rho)\alpha_d(\tau), \quad (15)$$

where $w_c=1$ in order to show explicitly that the cross-spectral degree of coherence is the weighted sum of the contribution of the collimated and diffuse components of the field. Considering the forward and backward specific intensity only, we have

$$\frac{W^{\pm}(\tau,\rho)}{W^{\pm}(\tau,0)}=\frac{W_c^{\pm}(\tau)}{W_c^{\pm}(\tau)}\frac{W_c^{\pm}(\tau)}{W_c^{\pm}(\tau)+W_d^{\pm}(\tau,0)}+\frac{W_d^{\pm}(\tau,\rho)}{W_d^{\pm}(\tau,0)}\frac{W_d^{\pm}(\tau,0)}{W_c^{\pm}(\tau)+W_d^{\pm}(\tau,0)}. \quad (16)$$

This can be cast in the form

$$w^{\pm}(\tau,\rho)=w_c^{\pm}\alpha_c^{\pm}(\tau)+w_d^{\pm}(\tau,\rho)\alpha_d^{\pm}(\tau), \quad (17)$$

where $w_c^{\pm}=1$. The coefficients α are weighting factors of the contribution of ballistic and diffuse components to the specific intensity. Then we can define the coherence lengths for the ballistic (superscript c) and diffuse (superscript d) components and for the forward (superscript $+$) and backward (superscript $-$) components of the specific intensity denoted by $l_{coh}^c, l_{coh}^d, l_{coh}^{c\pm}, l_{coh}^{d\pm}$, respectively. $l_{coh}^{\pm}$ corresponds to the beams in the forward or in the backward direction. We have obviously $l_{coh}^c=\infty$ and $l_{coh}^{c\pm}=\infty$. Thus these quantities will not be used in the following.

B. Coherence Length for the Forward Diffuse Component of the Radiation

We show in Fig. 3 the coherence length of the diffuse light propagating in the forward direction {ballistic component removed [Fig. 3(a)] and included [Fig. 3(b)]} versus the distance z from the medium interface. Different values of the anisotropy factor g are considered. We clearly see three regimes in Fig. 3(a).

- For $z<l_s$, the coherence length of the diffuse component increases. Note that this behavior is surprising at first glance because scattering tends to spread the specific

intensity and thus to decrease the coherence length. We have derived a simple model, based on the single-scattering approximation of the RTE, which describes this increase of the coherence length. This model is described in Section 5. In simple terms, the origin of this behavior is that rays propagating in a direction θ experience an exponential decay $\exp(-\tau/\cos\theta)$. It follows that the damping due to scattering acts as an angular filter that attenuates large-angle rays. Note that this is valid only in the single-scattering regime.

- For $l_s < z < l^*$, the coherence length decreases, owing to multiple scattering.
- For $z > l^*$, the coherence length reaches a constant value of the order of $\lambda/3$ (see Appendix B). This is a feature of the diffusive regime in a weakly absorbing medium, in which the radiation is quasi isotropic. The cross-spectral density is then given by Eq. (7).

C. Coherence Length for the Forward Component Including the Diffuse and Ballistic Radiation

When only the ballistic component of the specific intensity propagating in the forward direction is considered, the coherence length l_{coh}^{+} decreases exponentially with z (see Fig. 3). Actually, when z tends to 0, we have only a ballistic component (the diffuse component tends to 0), so that the coherence length tends to infinity. In contrast, for z of the order of $8l^*-10l^*$, the ballistic component is reduced, and the diffuse specific intensity is quasi isotropic. Hence l_{coh}^{+} tends to $\lambda/3$.

D. Coherence Length with Internal Reflections

So far, we have considered the coherence of the field in a random medium without reflections at the boundaries. In this subsection, we consider the coherence length when the refractive index n_2 is greater than 1 in order to study the effect of internal reflections. Figure 4 represents the coherence lengths l_{coh}^{d+} and l_{coh}^{+} associated with the forward component of the specific intensity as in Fig. 3 for an index of refraction $n_2 = 1.33$.

In Fig. 4(a) we see that for the diffuse coherence length l_{coh}^{d+} the variations are the same as in the case without internal reflections. But whatever the value of the anisotropy factor g, l_{coh}^{d+} tends to a unique limit, about 0.264λ when z tends to 0. To explain this observation, we plot in Fig. 5 the variations of the diffuse specific intensity versus θ for $z \ll l_s$ (i.e., at the entrance of the slab). We clearly see that the contribution of the whole reflection of I_d^- (see Section 5) dominates. The fact that the medium is semi-infinite produces a quasi-isotropic backscattered specific intensity I_d^- for all values of g. Thus the most important part of I_d^+ is a constant (independent of g), and the values of the diffuse coherence length are the same.

The full coherence length l_{coh}^{+} plotted in Fig. 4(b) does not tend to ∞ for $z \to 0$ for a weak anisotropy factor. The limit is finite, and thus the contribution of the collimated component is not dominating.

5. SINGLE-SCATTERING MODEL

To explain quantitatively the increase of the coherence length of the diffuse radiation at the beginning of the slab (i.e., for $z < l_s$), we derived a single-scattering model. We make the following assumptions:

1. $z \ll l_s$: single-scattering assumption.

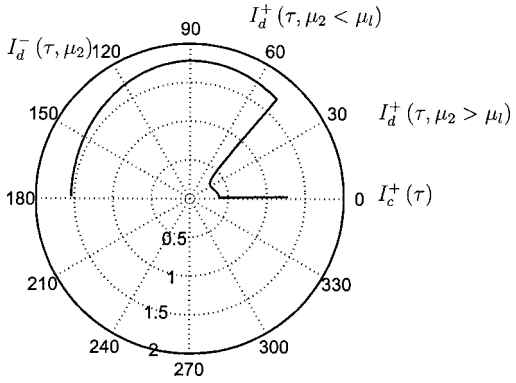

Fig. 5. Plot of the variations of the specific intensity at the entrance of the slab. Three zones can be identified: For $\mu_2 < 0$, the specific intensity is quasi isotropic owing to multiple scattering of light in a semi-infinite slab; for $0 < \mu_2 < \mu_l$, the specific intensity is also quasi isotropic owing to the whole reflection; and, for $\mu_2 > \mu_l$, there are two contributions, which are the partial reflection of I_d^- and the single scattering of the incident specific intensity.

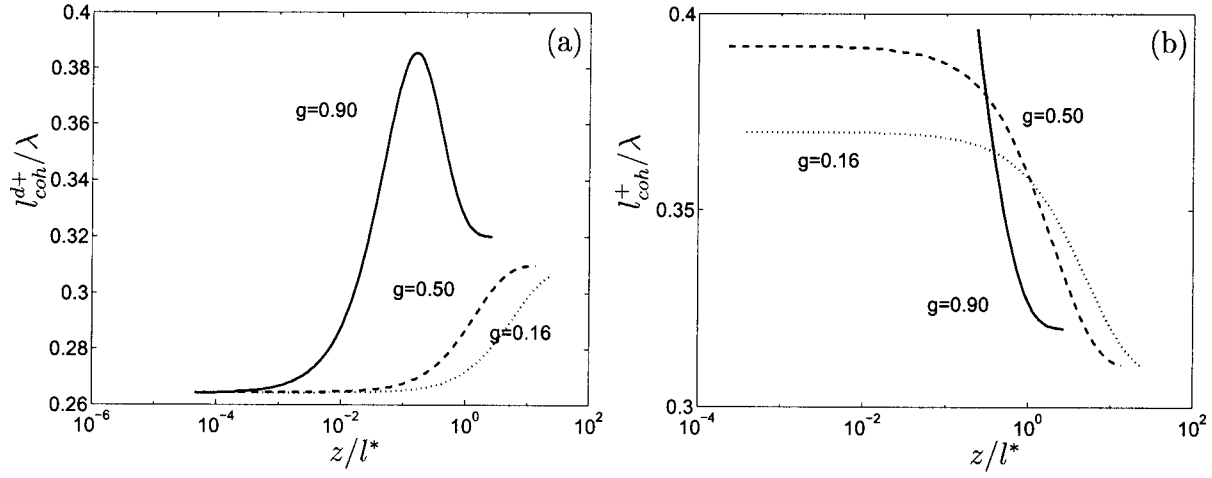

Fig. 4. Same as Fig. 3 with $n_2 = 1.33$.

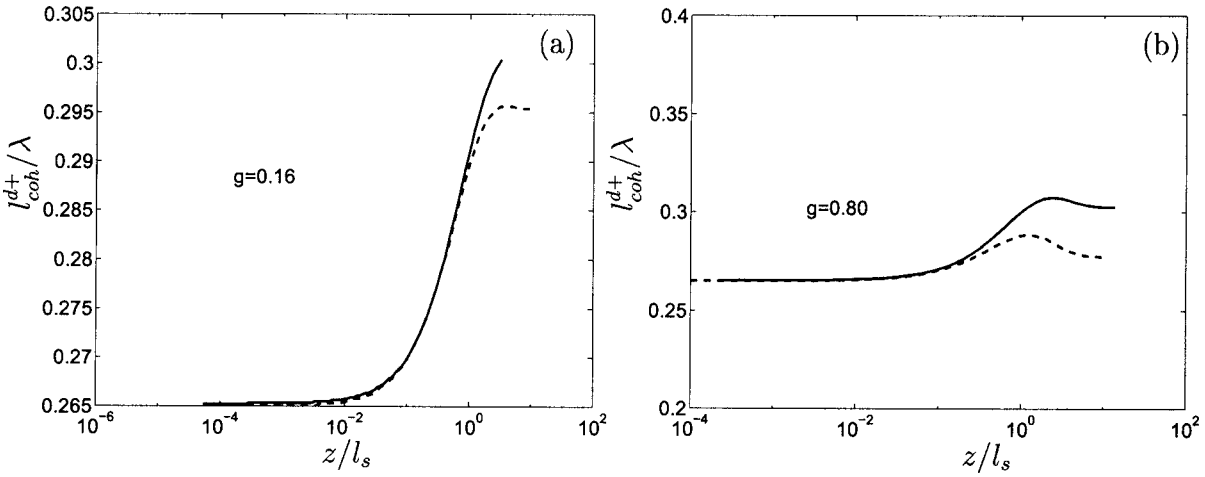

Fig. 6. Comparison between the single-scattering model (solid curve) and the whole numerical computation (dashed curve) for the diffuse spatial coherence length in the forward direction normalized by the wavelength versus the normalized distance z/l_s for two anisotropy factors [(a) $g=0.16$ and (b) $g=0.80$], an albedo $a=1$, and a refractive index $n_2=1.33$. We used a Henyey–Greenstein phase function. The scale for l_{coh}^{d+} is very small. The relative errors are about 2% for $z<8l^*-10l^*$.

2. $L^* \gg 1$: we study a semi-infinite medium. Thus the specific intensity at the entrance of the slab propagating in the backward direction will be quasi isotropic.

3. $a \approx 1$: The medium is not (or weakly) absorbing. This assumption allows us to write a flux conservation equation at the slab entrance.

4. $n_2 \geqslant 1$: The refractive index can be different from 1.

These assumptions allow us to derive an analytical form for the diffuse specific intensity propagating in the forward direction valid at the entrance of the slab (see Appendix C). We report in Fig. 6 the comparison between this analytical model and the full numerical computation for the coherence length. The relative errors are of the order of 2% for $z<8l^*-10l^*$. The very good agreement shows that the increase in the coherence of the diffuse field is indeed due to an angular filtering of the specific intensity.

6. CONCLUSION

In this paper, we have used the link between the specific intensity and the field spatial correlation function to analyze the field spatial coherence in a random medium. We have calculated numerically the specific intensity in a slab of a scattering medium using the RTE.[24] We have derived the spatial correlation function and the coherence length from the specific intensity. We have performed numerical experiments on systems with different properties and studied the coherence properties of both the ballistic and the diffuse components of the beam. In particular, we have studied the evolution of the coherence length versus the transport regime (single scattering, multiple scattering, diffusive). The crossover between the different regimes has been clearly seen, and the diffusive regime is reached for $z>8l^*-10l^*$. The study confirms that the RTE is an appropriate tool to study the transition between transport regimes.[25,26]

Finally, to reproduce the variations of the coherence length in the presence of reflections at the interface of the medium (i.e., when $n_2 \neq 1$), we have derived an analytical model based on the single-scattering approximation to compute the specific intensity. This model reproduces all the variations of the coherence length for distances from the interface of the order of the transport mean-free path.

APPENDIX A: WALTHER'S FORMULA

In this appendix, we invert Eq. (2) to show its equivalence with Walther's formula.[9] We introduce the decomposition $\mathbf{u}=\mathbf{u}_\perp+u_z\mathbf{e}_z$ and $\boldsymbol{\rho}=\boldsymbol{\rho}_\perp+\rho_z\mathbf{e}_z$, where $\mathbf{e}_z$ is a unit vector along the Oz axis. We note that

$$\mathrm{d}\Omega = \frac{\mathrm{d}u_x \mathrm{d}u_y}{|u_z|} = \frac{\mathrm{d}^2\mathbf{u}_\perp}{|u_z|}. \tag{A1}$$

Then Eq. (2) becomes

$$W(\mathbf{r},\boldsymbol{\rho}) = \int \frac{\exp(ik\rho_z u_z)}{|u_z|} I_\nu(\mathbf{r},\mathbf{u}) \exp(ik\boldsymbol{\rho}_\perp \cdot \mathbf{u}_\perp) \mathrm{d}^2\mathbf{u}_\perp. \tag{A2}$$

The variations of u_x and u_z are limited because $\|\mathbf{u}\|=1$. Nevertheless, we can avoid the problem by replacing the specific intensity with 0 for $\|\mathbf{u}\| \neq 1$ and thus perform the integral over the domain $[-\infty,+\infty]^2$. Then Eq. (A2) is a Fourier transform that can be inverted to yield

$$I_\nu(\mathbf{r},\mathbf{u}) = \left(\frac{k}{2\pi}\right)^2 |\mu| \int \exp(-ik\rho_z u_z) W(\mathbf{r},\boldsymbol{\rho}) \times \exp(-ik\boldsymbol{\rho}_\perp \cdot \mathbf{u}_\perp) \mathrm{d}^2\boldsymbol{\rho}_\perp, \tag{A3}$$

where $\mu=\cos\theta=u_z$. And then

$$I_\nu(\mathbf{r},\mathbf{u}) = \left(\frac{k}{2\pi}\right)^2 |\mu| \int W(\mathbf{r},\boldsymbol{\rho}) \exp(-ik\boldsymbol{\rho}\cdot\mathbf{u}) \mathrm{d}^2\boldsymbol{\rho}_\perp, \tag{A4}$$

which is the well-known Walther's formula.[9] Equation (A4) shows that the specific intensity is the Fourier transform of the cross-spectral density of the field or the Wigner transform of the field.

APPENDIX B: CALCULATION OF THE SPATIAL CORRELATION FUNCTION FOR AN ISOTROPIC SPECIFIC INTENSITY

We consider an isotropic specific intensity propagating in all directions. After integrating over the azimuthal angle φ, we obtain a specific intensity independent of μ. Thus we write

$$I(\tau,\mu)=I(\tau). \tag{B1}$$

Using this form in Eq. (6), we obtain

$$W(\tau,\rho)=I(\tau)\int_{-1}^{+1}\mathcal{J}_0\left(\frac{2\pi\rho}{\lambda}\sqrt{1-\mu^2}\right)\mathrm{d}\mu. \tag{B2}$$

First, we consider μ in the range $[0,+1]$ to compute the cross-spectral density in the forward direction $W^+(\tau,\rho)$. We define $X=2\pi\rho/\lambda$ and $u=\sqrt{1-\mu^2}$; thus $\mathrm{d}\mu=-u\mathrm{d}u/\sqrt{1-u^2}$. Equation (B2) now becomes

$$W^+(\tau,X)=I(\tau)\int_0^{+1}\mathcal{J}_0(Xu)\frac{u\mathrm{d}u}{\sqrt{1-u^2}}=I(\tau)\mathrm{sinc}(X). \tag{B3}$$

We also have the same result for the cross-spectral density accounting for wave propagation in the backward direction,

$$W^-(\tau,X)=I(\tau)\mathrm{sinc}(X), \tag{B4}$$

and, finally, for all directions, we have

$$W(\tau,X)=2I(\tau)\mathrm{sinc}(X). \tag{B5}$$

APPENDIX C: CALCULATION OF THE SPECIFIC INTENSITY IN THE SINGLE-SCATTERING MODEL

In this appendix, we derive the analytical expression for the specific intensity that has been used in Section 5. We denote the cosine of the critical angle by $\mu_l=\sqrt{1-n_1^2/n_2^2}$. μ_1 is the cosine of the angle θ_1 in the medium number **1**, and μ_2 is the one in the medium **2**, so that $n_1\sqrt{1-\mu_1^2}=n_2\sqrt{1-\mu_2^2}$. We decompose the specific intensity in three zones:

- For $-1<\mu_2<0$; assumption 2 (i.e., $L^*\gg 1$) allows us to write that $I_d^-(\tau,\mu_2)=XI_{inc}$ with X as an unknown variable.
- For $0<\mu_2<\mu_l$; there is total reflection of I_d^-. If we neglect the part of I_d^+ that was present without reflection, we have $I_d^+(\tau,\mu_2<\mu_l)=XI_{inc}$.
- For $\mu_l<\mu_2<1$; there is partial reflection of I_d^-. We now need to consider the part $I_d^{+\prime}$ of the specific intensity that was present without reflection. Thus we have $I_d^+(\tau,\mu_2>\mu_l)=X'I_{inc}+I_d^{+\prime}(\tau,\mu_2)$, where X' is another unknown.

Figure 5 presents the variations of the specific intensity at the entrance of the slab.

1. Computation of the Coefficients X and X'

Assumption 3 expresses that the flux entering the medium is equal to the flux leaving the scattering medium. Assumption 2 implies that this equality can be written only for $\tau=0$:

$$\underbrace{I_{inc}R_{12}(1)}_{\substack{\text{Flux from } \mathbf{1} \text{ to } \mathbf{2}\\ \text{reflected}}}+\underbrace{\int_{-1}^{0}-T_{21}^d(|\mu_1|)I_d^-(0,\mu_2)\mu_1\mathrm{d}\mu_1}_{\substack{\text{Flux from } \mathbf{2} \text{ to } \mathbf{1}\\ \text{transmitted}}}=\underbrace{I_{inc}}_{\substack{\text{Incident}\\ \text{flux}}}, \tag{C1}$$

where $R_{12}(|\mu_1|)$ is the energy Fresnel factor for the reflection from medium **1** to medium **2** that depends on μ_1. $T_{21}^d(|\mu_1|)$, which is the transmission factor for the specific intensity, is related to the Fresnel energy transmission factor $T_{21}(|\mu_1|)$ by[24]

$$T_{21}^d(|\mu_1|)=\frac{n_2^2}{n_1^2}T_{21}(|\mu_1|). \tag{C2}$$

Equation (C1) becomes

$$I_d^-(\tau,\mu_2)=\frac{1-R_{12}(1)}{\displaystyle\int_0^1 T_{21}^d(|\mu_1|)\mu_1\mathrm{d}\mu_1}I_{inc}=XI_{inc}. \tag{C3}$$

To compute X', we simply write the partial reflection of the diffuse specific intensity in the backward direction:

$$I_d^-(\tau,\mu_2)R_{21}(|\mu_2|)=X'I_{inc}, \tag{C4}$$

which leads to $X'=XR_{21}(|\mu_2|)$.

2. Computation of $I_d^{+\prime}(\tau,\mu_2)$

To compute the diffuse component of the specific intensity in the forward direction for $\mu_2>\mu_l$ and without reflection (i.e., $n_2=1$), we consider the RTE [Eq. (9)] where we split the specific intensity into its collimated and diffuse components.[25] Owing to assumption 1, we keep only the expression of the diffuse specific intensity for $-1<\mu_2<\mu_l$ in the phase function term:

$$\begin{aligned}\frac{a}{2}\int_{-1}^{1}p(\mu_2,\mu_2')I_d(\tau,\mu_2')\mathrm{d}\mu_2'&\approx\frac{a}{2}\int_{-1}^{\mu_l}p(\mu_2,\mu_2')XL_{inc}\mathrm{d}\mu_2'\\&=aI_{inc}J(\mu_2),\end{aligned} \tag{C5}$$

with

$$J(\mu_2)=\frac{X}{2}\int_{-1}^{\mu_l}p(\mu_2,\mu_2')\mathrm{d}\mu_2'.$$

For the collimated component of the specific intensity, we need to take into account the energy Fresnel transmission factor $T_{12}(1)$:

$$I_c^+(\tau)=T_{12}(1)\exp(-\tau). \tag{C6}$$

Thus, Eq. (9) becomes

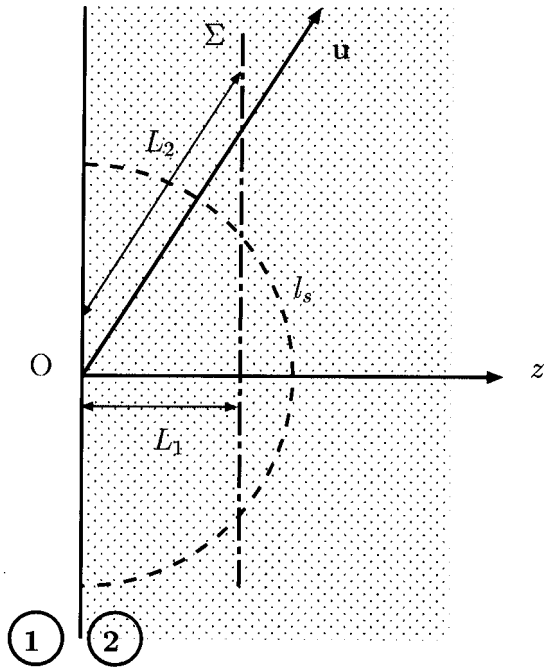

Fig. 7. Geometrical filtering effect on the coherence length.

$$\mu\frac{\partial I_d^{+\prime}}{\partial\tau}(\tau,\mu_2)+I_d^{+\prime}(\tau,\mu_2)=aI_{inc}J(\mu_2)+\frac{a}{2}p(\mu_2,1)T_{12}(1)I_{inc}\times\exp(-\tau). \tag{C7}$$

The boundary condition is given by

$$I_d^{+}(0,\mu_2)=0. \tag{C8}$$

The solution of Equations (C7) and (C8) yields an analytical form of the specific intensity:

$$I_d^{+\prime}(\tau,\mu_2)=\frac{aI_{inc}}{2(1-\mu_2)}\left\{2I(\mu_2)(1-\mu_2)+p(\mu_2,1)T_{12}(1)\times\exp(-\tau)-[2I(\mu_2)(1-\mu_2)+p(\mu_2,1)T_{12}(1)]\times\exp\left(-\frac{\tau}{\mu_2}\right)\right\}. \tag{C9}$$

The key feature that explains the increase of the coherence length is the damping factor $\exp(-\tau/\mu_2)$ that acts as an angular filter. Figure 7 shows the origin of this effect. We consider two rays propagating along different directions. Rays propagate along a length L/μ_2 in the scattering medium and therefore experience an attenuation $\exp(-\tau/\mu_2)$. This is the same effect as the attenuation of sunlight through the atmosphere. Light is strongly attenuated at sunset ($\mu_2 \ll 1$) and almost fully transmitted at noon ($\mu_2=1$). It follows that this term acts as an angular filter. Finally, Eq. (C9) gives the diffuse specific intensity in the forward direction. The coherence length can thus be easily deduced.

ACKNOWLEDGMENTS

This work is supported by the European Integrated Project Molecular Imaging, under contract LSHG-CT-2003-503 259, and by the Engineering and Physical Sciences Research Council grant GR/R86201/01. We acknowledge helpful discussions with M. A. Alonso.

Corresponding author Rémi Carminati's e-mail address is remi.carminati@em2c.ecp.fr.

REFERENCES

1. P. Sebbah, *Waves and Imaging through Complex Media* (Kluwer Academic, 2001).
2. A. Ishimaru, *Wave Propagation and Scattering in Random Media* (IEEE, 1997).
3. L. A. Apresyan and Y. A. Kravtsov, *Radiation Transfer—Statistical and Wave Aspects* (Gordon & Breach, 1996).
4. F. C. MacKintosh and S. John, "Diffusing-wave spectroscopy and multiple scattering of light in correlated random media," Phys. Rev. B **40**, 2383–2406 (1989).
5. V. I. Tatarskii, *Effects of the Turbulent Atmosphere on Wave Propagation* (U.S. Department of Commerce, 1971).
6. L. C. Andrews and R. L. Philips, *Laser Beam Propagation through Random Media* (SPIE, 1998).
7. S. A. Ponomarenko, J.-J. Greffet, and E. Wolf, "The diffusion of partially coherent beams in turbulent media," Opt. Commun. **208**, 1–8 (2002).
8. D. Huang, E. A. Swanson, C. P. Lin, J. S. Schuman, W. G. Stinson, W. Chang, M. R. Hee, T. Flotte, K. Gregory, C. A. Puliafito, and J. G. Fujimoto, "Optical coherence tomography," Science **254**, 1178–1181 (1991).
9. A. Walther, "Radiometry and coherence," J. Opt. Soc. Am. **58**, 1256–1259 (1968).
10. H. M. Pedersen, "Exact geometrical theory of free-space radiative energy transfer," J. Opt. Soc. Am. A **8**, 176–185 (1991).
11. H. M. Pedersen, "Exact geometrical theory of free-space radiative energy transfer: errata," J. Opt. Soc. Am. A **8**, 1518–1518 (1991).
12. E. Wolf, "Radiometric model for propagation of coherence," Opt. Lett. **19**, 2024–2026 (1994).
13. M. Alonso, "Radiometry and wide-angle wave fields. I. Coherent fields in two dimensions," J. Opt. Soc. Am. A **18**, 902–909 (2001).
14. M. Alonso, "Radiometry and wide-angle wave fields. II. Coherent fields in three dimensions," J. Opt. Soc. Am. A **18**, 910–918 (2001).
15. L. Mandel and E. Wolf, *Optical Coherence and Quantum Optics* (Cambridge U. Press, 1995).
16. S. M. Rytov, Y. A. Kravtsov, and V. I. Tatarskii, *Principles of Statistical Radiophysics* (Springer-Verlag, 1989), Vol. 4.
17. Y. N. Barabanenkov, "On the spectral theory of radiation transport equations," Sov. Phys. JETP **29**, 679–684 (1969).
18. L. Ryzhik, G. Papanicolaou, and J. B. Keller, "Transport equations for elastic and other waves in random media," Wave Motion **24**, 327–370 (1996).
19. S. Chandrasekhar, *Radiative Transfer* (Dover, 1960).
20. R. G. Littlejohn and R. Winston, "Generalized radiance and measurement," J. Opt. Soc. Am. A **12**, 2736–2743 (1995).
21. R. Winston and R. G. Littlejohn, "Measuring the instrument function of radiometers," J. Opt. Soc. Am. A **14**, 3099–3101 (1997).
22. L. Roux, P. Mareschal, N. Vukadinovic, J.-B. Thibaud, and J.-J. Greffet, "Scattering by a slab containing randomly located cylinders: comparison between radiative transfer and electromagnetic simulation," J. Opt. Soc. Am. A **18**, 374–384 (2001).

23. G. E. Thomas and K. Stamnes, *Radiative Transfer in the Atmosphere and Ocean* (Cambridge U. Press, 1999).
24. R. Elaloufi, R. Carminati, and J.-J. Greffet, "Time-dependent transport through scattering media: from radiative transfer to diffusion," J. Opt. A, Pure Appl. Opt. **4**, S103–S108 (2002).
25. R. Elaloufi, R. Carminati, and J.-J. Greffet, "Diffusive-to-ballistic transition in dynamic light transmission through thin scattering slabs: a radiative transfer approach," J. Opt. Soc. Am. A **21**, 1430–1437 (2004).
26. R. Carminati, R. Elaloufi, and J.-J. Greffet, "Beyond the diffusion-wave spectroscopy model for the temporal fluctuations of scattered light," Phys. Rev. Lett. **92**, 213903 (2004).